



2003

# Superconductivity, critical current density, and flux pinning in $\text{MgB}_{2-x}(\text{SiC})_{x/2}$ superconductor after SiC nanoparticle doping

S X. Dou

*University of Wollongong*, shi@uow.edu.au

A. V. Pan

*University of Wollongong*, pan@uow.edu.au

S. Zhou

*University of Wollongong*

M. Ionescu

*University of Wollongong*, mionescu@uow.edu.au

Xiaolin Wang

*University of Wollongong*, xiaolin@uow.edu.au

*See next page for additional authors*

<http://ro.uow.edu.au/engpapers/90>

## Publication Details

This article originally appeared as: Dou, SX, Pan, AV, Zhou, S, Ionescu, M, Wang, XL, Horvat, J, Liu, HK & Munroe, PR, Superconductivity, critical current density, and flux pinning in  $\text{MgB}_{2-x}(\text{SiC})_{x/2}$  superconductor after SiC nanoparticle doping, *Journal of Applied Physics*, 2003, 94(3), 1850-1856, and may be found [here](#). Copyright (2003) American Institute of Physics. This article may be downloaded for personal use only. Any other use requires prior permission of the author and the American Institute of Physics.

---

**Authors**

S X. Dou, A. V. Pan, S. Zhou, M. Ionescu, Xiaolin Wang, J. Horvat, Hua-Kun Liu, and P. R. Munroe

# Superconductivity, critical current density, and flux pinning in $\text{MgB}_{2-x}(\text{SiC})_{x/2}$ superconductor after SiC nanoparticle doping

S. X. Dou, A. V. Pan, S. Zhou, M. Ionescu, X. L. Wang, J. Horvat, and H. K. Liu  
*Institute for Superconducting and Electronic Materials, University of Wollongong, Wollongong,  
Northfields Avenue, NSW 2522, Australia*

P. R. Munroe

*Electron Microscopy Unit, University of New South Wales, Sydney, NSW 2052, Australia*

(Received 25 November 2002; accepted for publication 29 April 2003)

We investigated the effect of SiC nanoparticle doping on the crystal lattice structure, critical temperature  $T_c$ , critical current density  $J_c$ , and flux pinning in  $\text{MgB}_2$  superconductor. A series of  $\text{MgB}_{2-x}(\text{SiC})_{x/2}$  samples with  $x=0-1.0$  were fabricated using an *in situ* reaction process. The contraction of the lattice and depression of  $T_c$  with increasing SiC doping level remained rather small most likely due to the counterbalancing effect of Si and C co-doping. The high level Si and C co-doping allowed the creation of intragrain defects and highly dispersed nanoinclusions within the grains which can act as effective pinning centers for vortices, improving  $J_c$  behavior as a function of the applied magnetic field. The enhanced pinning is mainly attributable to the substitution-induced defects and local structure fluctuations within grains. A pinning mechanism is proposed to account for different contributions of different defects in  $\text{MgB}_{2-x}(\text{SiC})_{x/2}$  superconductors. © 2003 American Institute of Physics. [DOI: 10.1063/1.1586467]

## I. INTRODUCTION

Extensive research efforts have been made towards increasing the critical temperature ( $T_c$ ) in  $\text{MgB}_2$  since superconductivity in this compound was discovered.<sup>1</sup> The most commonly used procedures are high pressure treatment and element substitutions as summarized in a recent review article by Buzea and Yamashita,<sup>2</sup> and references therein. It appears that all element substitutions cause crystal lattice contraction and reduced  $T_c$ . The elements which do not significantly reduce  $T_c$  are Zn, Si, and Li. However, all element substitutions reported so far are limited to single element doping. Because of the rigid lattice structure and small number of elements in the  $\text{MgB}_2$  compound the level of substitution is substantially restricted, otherwise  $T_c$  would be strongly depressed. Furthermore, the majority of studies on substitution were carried out to replace Mg with exception of recent work on C (Refs. 3, 4) and Si (Ref. 5) substitutions aimed at replacing B.

Another important goal of substitution is enhancement of pinning in  $\text{MgB}_2$ . In spite of impressive progress on improving the critical current density ( $J_c$ ) (Refs. 6–12) at temperatures above 20 K, which is considered to be the benchmark operating temperature for this material,  $J_c$  rapidly drops with increasing magnetic field ( $H$ ) due to its poor pinning ability. If  $\text{MgB}_2$  is to be useful in high fields, the flux pinning strength must be improved. Attempts have been made to enhance the flux pinning by oxygen alloying in  $\text{MgB}_2$  thin films<sup>13</sup> and by proton irradiation of  $\text{MgB}_2$  powder,<sup>14</sup> which led to an encouraging improvement of both irreversibility field ( $H_{\text{irr}}$ ) and  $J_c(H)$ . The question is whether one can introduce effective pinning centers into  $\text{MgB}_2$  by chemical doping. Numerous attempts have been made to improve flux pinning using this procedure. The re-

sults for doping into  $\text{MgB}_2$  reported so far are largely limited to addition rather than substitution of the doping elements. Additives appeared to be ineffective for pinning enhancement at high temperatures.<sup>15–17</sup> However, if doping elements are substituted into, instead added to  $\text{MgB}_2$  crystals, pinning properties can be much improved by induction of a net of intragranular defects due to crystal lattice distortions and local fluctuations of the superconducting order parameter. Both can strongly contribute to pinning. Indeed, pinning reinforcement research in  $\text{MgB}_2$  has to be focused on intragranular pinning, as the weak-link problem is insignificant for this material,<sup>18,19</sup> unlike for high- $T_c$  systems. Therefore, it is necessary to have a high doping level and multielement substitution, creating effective pinning sites but not lowering  $T_c$  dramatically. Indeed, for  $\text{MgB}_2$ , the boron plane is responsible for superconductivity, so that it is desirable for substitution to take place in B positions, which would induce local fluctuations of the superconducting order parameter.

In our previous work,<sup>20</sup> we doped  $\text{MgB}_2$  with SiC nanoparticle powder, producing  $\text{MgB}_2(\text{SiC})_x$  compound where  $x=0-0.34$ . It was found that the added SiC was *dissolved* within the crystal lattice; that Si and C co-substitution resulted in a surprisingly modest reduction of  $T_c$  (only 2.6 K for  $x=0.34$ ), and that vortex pinning was significantly increased, dramatically improving  $J_c(H)$  behavior.<sup>20</sup> However, from the doping procedure it was difficult to estimate the level of substitution with increasing  $x$ . Excessive secondary phases also appeared as 10 nm inclusions inside the  $\text{MgB}_2$  grains. It was not quite clear what was the predominating factor for the enhanced pinning: the substitution or the inclusions. In this detailed work, we report not only the influence of SiC co-substitution for B in the form of  $\text{MgB}_{2-x}(\text{SiC})_{x/2}$ , with  $x$  varying from 0 to 1, on different aspects of supercon-

ductivity in the material, but also show that the substitution is primarily responsible for the improved  $J_c(H)$  performance, whereas impurities (inclusions) play an assisting role, apparently making a considerable contribution to the pinning of vortices at relatively low fields.

In the next section we describe the sample preparation procedure and experimental details. In Sec. III, we show the effect of substitution on  $\text{MgB}_2$  crystal lattice contraction and phase composition (Sec. III A); in Sec. III B we discuss reasons for the small critical temperature degradation for relatively high SiC-doping level, and show that  $T_c$  degradation due to the substitution is similar to the effect of hydrostatic pressure applied to  $\text{MgB}_2$ ; in Sec. III C we mainly deal with critical current density behavior as a function of the applied field and temperature, providing evidence for the improved performance as a result of the SiC doping procedure. We also propose a quantitative pinning mechanism to account for the  $J_c(H)$  behavior. In the last section we summarize the results obtained and our conclusions.

## II. EXPERIMENT

$\text{MgB}_2$  samples were prepared by an in-situ reaction, which has been previously described in detail.<sup>21</sup> Powders of magnesium (99%) and amorphous boron (99%) were well mixed with powder of SiC nanoparticles, varying from 10 nm to 100 nm in size, with an atomic ratio of  $\text{MgB}_{2-x}(\text{SiC})_{x/2}$ , where  $x=0, 0.04, 0.1, 0.2, 0.3, 0.5, 0.65, 0.8, \text{ and } 1.0$ . The mixed powders were packed into Fe tubes. The composite tubes were groove-rolled, sealed in a Fe tube, and then directly heated in a furnace preset to  $950^\circ\text{C}$ , for 1 h in flowing high purity Ar. This was followed by quenching to liquid nitrogen temperature.

X-ray-powder diffraction (XRD) measurements were performed on undoped and SiC-doped samples. The x-ray scans were recorded using  $\text{CuK}\alpha = 1.5418 \text{ \AA}$ , and indexed within the space group  $P6/mmm$ . Microstructure and micro-composition were characterized using a scanning electron microscope (SEM) and a transmission electron microscope (TEM) equipped with an energy dispersive x-ray spectroscopy analyzer (EDS) and mapping analysis. The magnetization as a function of temperature  $T$  and magnetic field  $H$  applied along the longest sample dimension was measured using Quantum Design Magnetic Property and Physical Property Measurement Systems within the field range  $|H| \leq 9 \text{ T}$ , and within the temperature range of  $5 \text{ K} \leq T \leq 30 \text{ K}$ . A magnetic  $J_c$  was derived from the half-width of magnetization loops  $\Delta M = (|M^+| + |M^-|)/2$  ( $M^+$  and  $M^-$  are descending and ascending branches of the magnetization loop, respectively), using the following critical state model formula:  $J_c = k10\Delta M/d$ , where  $k = 12w/(3w-d)$  is a geometrical factor, with  $d$  and  $w$  being sample thickness and width, respectively. All the samples were of a similar rectangular shape and size. Because of the strong thermo-magnetic flux-jump instabilities the low field  $J_c$  could not be measured at  $T \leq 10 \text{ K}$ .

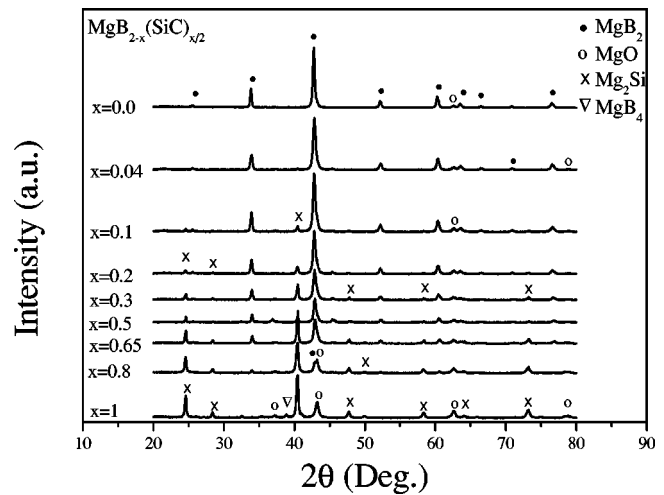


FIG. 1. X-ray diffraction patterns for all the measured  $\text{MgB}_{2-x}(\text{SiC})_{x/2}$  samples.

## III. RESULTS AND DISCUSSION

### A. Structural change of $\text{MgB}_2$ due to substitution

Figure 1 shows x-ray diffraction patterns for the series of  $\text{MgB}_{2-x}(\text{SiC})_{x/2}$  samples where  $x=0-1.0$ . For the in-phase reflection which occurs between  $2\theta=33^\circ$  and  $2\theta=34^\circ$  indexed as (100), the centroid of the peak clearly shifts to higher  $2\theta$  values with increasing  $x$ , indicating a contraction of the  $a$ -axis of the crystal lattice. For the (002) reflection peak, which occurs between  $2\theta=51^\circ$  and  $2\theta=52^\circ$ , the shift to higher  $2\theta$  values with increasing  $x$  is relatively small. The change of the lattice parameters,  $a$  and  $c$  of the hexagonal  $\text{AlB}_2$ -type structure of  $\text{MgB}_2$  were calculated using the peak shifts shown in Fig. 2.

At lower doping level ( $x < 0.1$ ), the sample consists of a major phase with the  $\text{MgB}_2$  structure. At  $x \geq 0.1$  minority phase  $\text{Mg}_2\text{Si}$  and trace amount of  $\text{MgO}$  were identified. The amount of these nonsuperconducting phases was increased with increasing SiC doping level. At  $x=0.1-0.2$ , the minority phase  $\text{Mg}_2\text{Si}$  occupied about a 10% volume fraction. This minority phase increased to about a 30% volume fraction for  $0.3 \leq x \leq 0.5$ . At  $x=0.65$ , the amount of nonsuperconducting phases already exceeded  $\text{MgB}_2$ . At  $x=1.0$ , the reflection

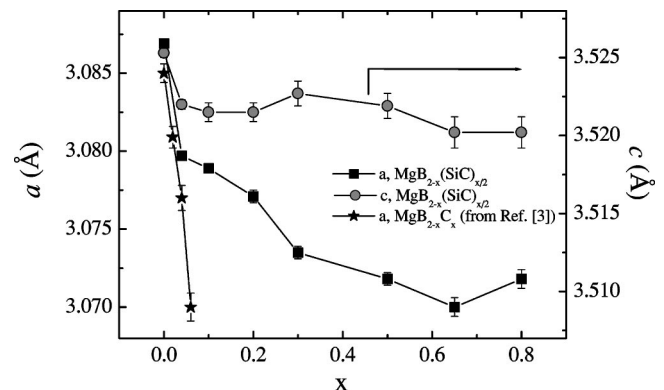


FIG. 2. Lattice parameters  $a$  and  $c$  as a function of the nominal SiC content  $x$ . For comparison, the variation of the  $a$ -axis for the single element C substitution for B taken from Ref. 3 is also shown.

peaks (100) and (002) for the  $\text{MgB}_2$  structure disappeared, and the sample consists of multiphases which can no longer be indexed as the  $\text{MgB}_2$  structure (Fig. 1).

Both crystal lattice axes are sharply reduced at low doping levels  $x \leq 0.04$  (Fig. 2), nevertheless the sample overwhelmingly remained single phase (Fig. 1). After a sharp contraction, the  $a$ -axis continues to moderately decrease with increasing doping level until the nominal composition  $x = 0.65$  is reached. At the same time, the  $c$ -axis remains almost constant. The negligible  $c$ -axis variations are within the experimental error. These results suggest that at a low doping level the SiC-dopant is to a large extent dissolved in the  $\text{MgB}_2$  crystal lattice. As the doping level increases the substitution effect slows down, but it can still be quite effective up to  $x \approx 0.5$ , where the  $a$ -axis change reaches a quasiplateau (Fig. 2). Furthermore, the slow variation in the  $a$ -axis with increasing SiC doping level most probably indicates that B was substituted by C and Si. In comparison, pure C substitution for B resulted in a reduction of the  $a$ -axis from 3.085 to 3.070 Å at  $x = 0.065$  (Ref. 3) (Fig. 2), while the co-doping of Si and C into the B site reached a similar level of  $a$ -axis reduction at the nominal composition  $x = 0.65$ . This is an order of magnitude higher than for the single element doping (Fig. 2). It is clear that the Si and C substitution raised the saturation level considerably. This is probably due to the fact that the average atomic radius of C (0.91 Å) and Si (1.46 Å) closely matches that of B (1.17 Å). Therefore, this co-doping counterbalanced the negative effect of the single element doping.<sup>20</sup> The formation of  $\text{Mg}_2\text{Si}$  phase could not consume all of the Si, because the crystal lattice would then show a similar contraction to the one obtained for the single element C-doping<sup>3</sup> (see Fig. 2) accompanied by a strong decrease of  $T_c$ .<sup>3</sup> This was not observed in our experiment (see Sec. III B).

The simultaneous incorporation of C and Si into the lattice structure is also supported by energy dispersive x-ray spectroscopy analysis on single grains of  $\text{MgB}_2$ . The analysis clearly shows that Si and C coexist with Mg and B within the same grain (Fig. 3). Moreover, the  $(\text{Si} + \text{C})/\text{B}$  ratio obtained for samples having different doping levels quantitatively correlates with the corresponding nominal doping level of the sample. However, we observed local variations of the signal intensity for C and Si across each analyzed grain, suggesting very local variations in the substitution level and making a qualitative assessment impossible. This is in contrast to Mg and B, which appear to be rather uniformly distributed across each analyzed grain. In Fig. 3, we present the spectral analysis for two samples having  $x = 0.2$  (a) and  $x = 0.5$  (b). Note that the B-peak intensity became comparable to the intensities of Si- and C-peaks for the higher doping level sample [Fig. 3(b)], pointing out that Si and C replace B within the  $\text{MgB}_2$  grains.

The spectral analysis clearly shows an O peak within the  $\text{MgB}_2$  grains (Fig. 3). The oxygen itself could be brought into the material by SiC dopant which can absorb oxygen and moisture during storage. There are two reasons why an oxygen peak appears in the EDS spectrum within the grains. First, it might be due to oxygen alloying in boron layers, which was reported to result in strong pinning in the  $\text{MgB}_2$

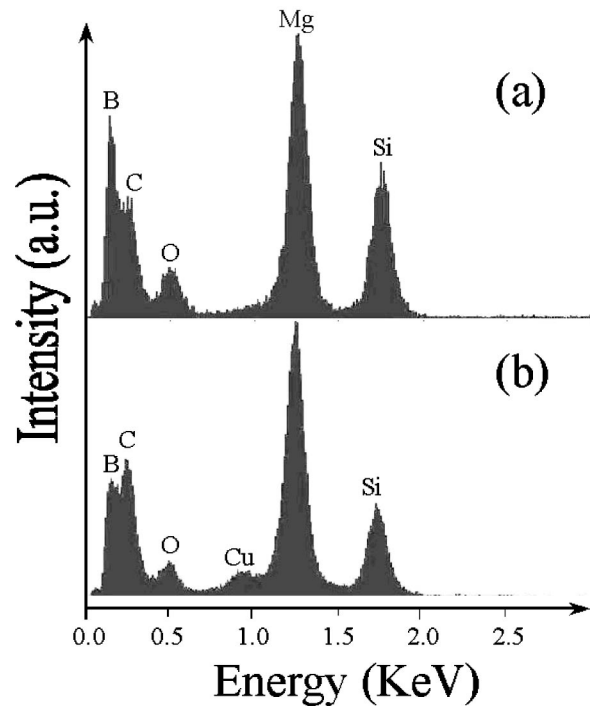


FIG. 3. The EDS analysis results taken on single grains of  $x = 0.2$  (a) and  $x = 0.5$  (b) samples. Note the coexistence of Si, C, B, and Mg within each individual grain. A small Cu-peak in (b) appeared due to the background signal from the sample holder.

thin films.<sup>13</sup> Secondly, the oxygen peak may be attributable to the presence of  $\text{MgO}$  nanosize inclusions formed within the grains.

## B. Effect of SiC-doping on $T_c$

Figure 4 shows the onset of critical temperature  $T_c^{\text{onset}}$  as a function of the doping level, as obtained by zero-field cooled magnetization  $M$  measurements at  $H = 25$  Oe. The  $M(T)$  behavior, as well as the increase of the transition width with increasing doping level, is similar to that exhibited in our preceding work.<sup>20</sup> The onset was defined at sus-

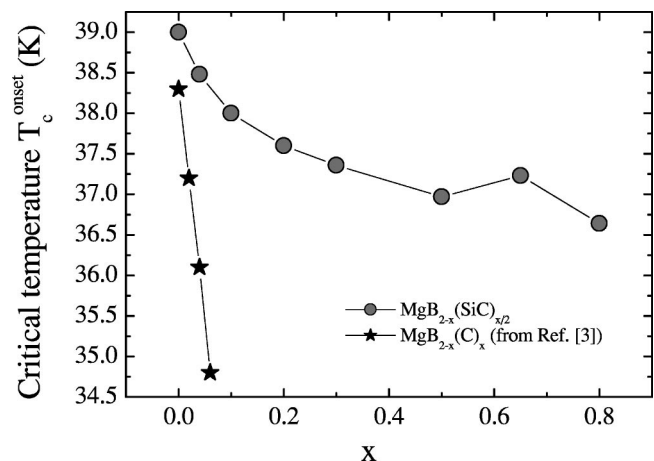


FIG. 4. The critical temperature onset  $T_c^{\text{onset}}$  vs the doping level for all the measured samples. For comparison,  $T_c$  for the single element doping taken from Ref. 3 is also shown.

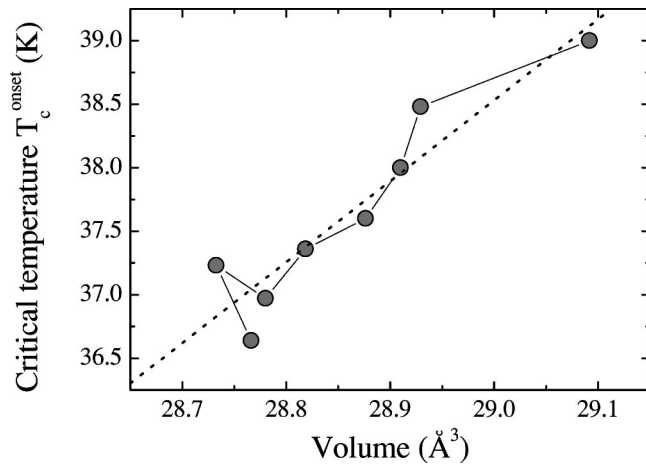


FIG. 5. The crystal lattice unit cell volume change vs  $T_c^{\text{onset}}$  for the investigated doping range. The dotted line is a linear fit to the data.

ceptibility  $\chi_{\text{dc}} = -5 \times 10^{-5} \text{ emu/cm}^3$ . For the undoped sample,  $T_c^{\text{onset}} \approx 38.98 \text{ K}$ . For the doped samples,  $T_c^{\text{onset}}$  decreases almost monotonically with increasing doping level. Surprisingly, the degradation of  $T_c^{\text{onset}}$  slows down, and likely reaches a quasiplateau for  $x \geq 0.5$ , whereas for samples having  $x \geq 1$  the bulk superconductivity vanishes, at least in the measured temperature range of  $5 \text{ K} \leq T \leq 45 \text{ K}$ . The total  $T_c^{\text{onset}}$  drop is only 2.4 K for the superconducting samples with an SiC doping level up to  $x = 0.8$  (nominal composition). In contrast,  $T_c$  was depressed by almost 7 K in the case of pure C doping in  $\text{MgB}_{2-x}\text{C}_x$  with  $x = 0.2$ ;<sup>3</sup>  $T_c$  was reduced by about 0.5 K in the case of Si substitution in  $\text{MgB}_{2-x}\text{Si}_x$  with  $x = 0.05$ .<sup>5</sup> The latter result, as well as our preliminary experiments on Si-doping suggest that silicon substitution has also a stronger effect on the depression of  $T_c$  compared to the case of the SiC-doping.

These results may also support the idea of a counterbalance effect caused by C and Si co-substitution, producing the

higher  $T_c$  tolerance to  $\text{MgB}_2$  structural changes induced by SiC doping. It is evident that the co-doping counterbalanced the negative effect on  $T_c$  of the single element doping.

As widely discussed in the literature, there are two factors that influence  $T_c$ : lattice structure change and electronic structure change.<sup>2</sup> From pressure experiments, it was found that  $T_c$  decreases almost linearly with decreasing lattice volume (see the review paper,<sup>2</sup> and references therein). As far as the lattice volume change is concerned, the C substitution for B would cause contraction of the crystal lattice and, hence, reduction of the unit cell volume; whereas the Si substitution for B would lead to expansion of the lattice and increase of the unit volume. Thus, it is plausible for  $\text{MgB}_2$  to accommodate larger amounts of C and Si than in the case of the single element doping. The larger level of substitution could bring forward an additional  $T_c$  suppressing factor. The reduction may occur not only due to the lattice contraction, but also due to alteration of the electron configuration with the doping. To assess each of the possible contributions, we have plotted  $T_c^{\text{onset}}$  vs crystal lattice unit cell volume as shown in Fig. 5. The resulting dependence is rather linear. Similar linear dependencies have been obtained for pressure experiments on pure  $\text{MgB}_2$  material.<sup>2</sup> Therefore, this similarity enables us to conclude that our co-substitution produces the same effect on  $T_c$  as in the case of the pressure induced volume decrease, indicating that the volume (structural) factor plays the dominant role in affecting  $T_c$  in the Si and C co-doped  $\text{MgB}_2$  system.

### C. Effect of SiC-doping on $J_c$ and pinning

Figure 6 shows the  $J_c(H)$  curves for selected samples at  $T = 5 \text{ K}$  (a),  $10 \text{ K}$  (b),  $20 \text{ K}$  (c), and  $30 \text{ K}$  (d). The most striking feature shown in this figure is that  $J_c(H)$ -curves for samples with a wide range of doping cross the curve of the pure ( $x = 0$ )  $\text{MgB}_2$  sample, exhibiting significantly higher critical current densities at higher applied fields. This is con-

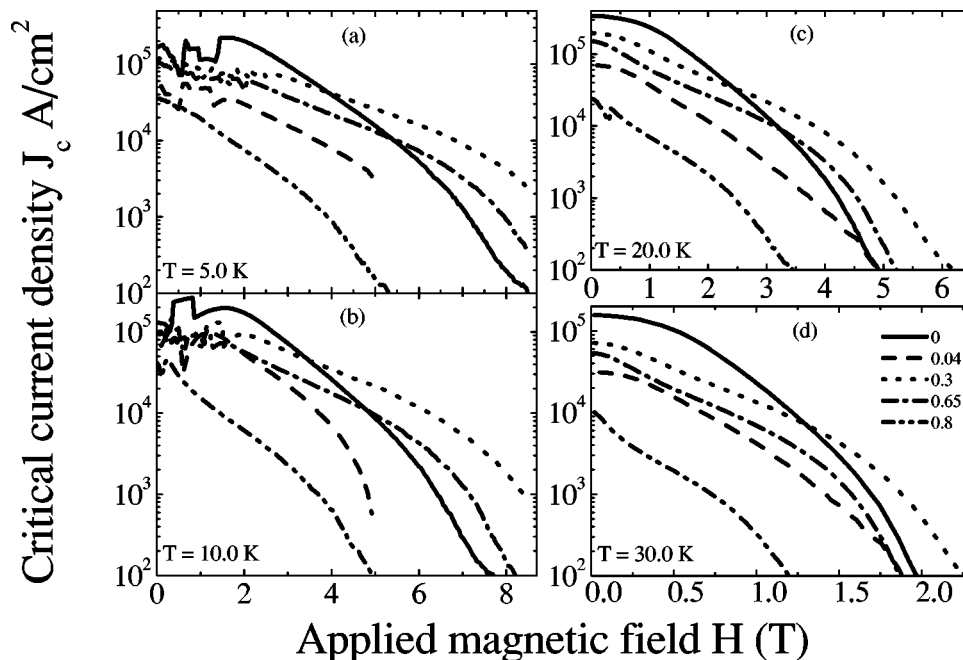


FIG. 6. Effect of SiC doping on  $J_c(H)$  behavior of selected investigated samples compared to the pure  $\text{MgB}_2$  sample at  $T = 5 \text{ K}$  (a),  $10 \text{ K}$  (b),  $20 \text{ K}$  (c), and  $30 \text{ K}$  (d).

sistent with our first report on  $\text{MgB}_2(\text{SiC})_x$  samples.<sup>20</sup> The behavior is valid for the samples having the doping range of  $0.1 \leq x \leq 0.65$ , however  $J_c(H)$ -curves in Fig. 6 are not shown for all measured samples for clarity. For example, samples in the doping range of  $0.1 \leq x \leq 0.3$  show almost indistinguishable  $J_c(H)$ -behavior. It is important further to note at least two more interesting features revealed by our study. (i) The sample having  $x = 0.65$ , showed a relatively good  $J_c(H)$  performance in high fields and  $T < 30$  K (Fig. 6), but what is striking that it has at least a 50% volume fraction of *nonsuperconducting phase*, according to the XRD results shown in Fig. 1. (ii) At low doping levels  $x < 0.1$  the  $J_c(H)$  behavior is surprisingly not only worse than that for the pure sample, but also for the higher doping level samples ( $0.1 \leq x < 0.8$ ). Below, we shall discuss possible reasons for the  $J_c(H)$  behavior shown in Fig. 6 and indicate possible pinning mechanisms responsible for this behavior.

First, for our samples we rule out the densification effect reported in the literature<sup>15,16</sup> for different doping materials, which leads to a  $J_c$  increase in rather low fields and temperatures. This would mean that, instead of introducing pinning into  $\text{MgB}_2$ , doping would help increase the density of the material, which would increase the effective cross-sectional area for supercurrent transport and reduce its percolative flow. In contrast to Refs. 15 and 16, but similarly to the work on  $\text{Y}_2\text{O}_3$  nanoparticle doping,<sup>17</sup> SiC doping showed no densification effect as evidenced by the fact that the density of our samples is independent of the doping level and equal to approximately  $1.2 \text{ g/cm}^3$ . This is less than 50% of the theoretical density for this material,  $2.63 \text{ g/cm}^3$ . This lack of densification is probably because the melting temperature of SiC is very high, and SiC would not act as a sintering aid in the temperature range of  $800\text{--}950^\circ\text{C}$ . Thus, densification can not be claimed responsible for the improved  $J_c(H)$  behavior at high fields in our doped samples.

In order to describe the origin of the pinning enhancement which is responsible for the observed  $J_c(H)$  behavior, it is necessary to recognize the unique features of SiC doping emphasized in the previous sections. It primarily takes place in the form of substitution, but addition takes place as well especially at higher doping levels while in works reported in the literature<sup>3–5,15–17</sup> most element doping was in the form of additives, thus either not incorporated into the crystal lattice or incorporated to a lesser extent than in our work. This indicates that  $J_c$  is very sensitive to the way impurities are introduced. A question arises, what kind of implications does *substitution* have on the pinning properties of the material?

As already shown in Fig. 2, substitution causes the crystal lattice parameters to contract inducing local lattice strains in the  $\text{MgB}_2$  crystal framework. This would create not only local fluctuations of the superconducting order parameter, but also cause the appearance of a number of crystal defects. Indeed, our transmission electron microscopy (TEM) investigations clearly show a large number of dislocations within each  $\text{MgB}_2$  grain [Fig. 7(a)], which are similar to those shown in our previous report.<sup>20</sup> Dislocations are known to serve as strong pinning centers.<sup>22</sup> The very limited structural study of the  $\text{MgB}_2$  superconductor available in the literature has indicated that pure  $\text{MgB}_2$  has only very few atomic-scale

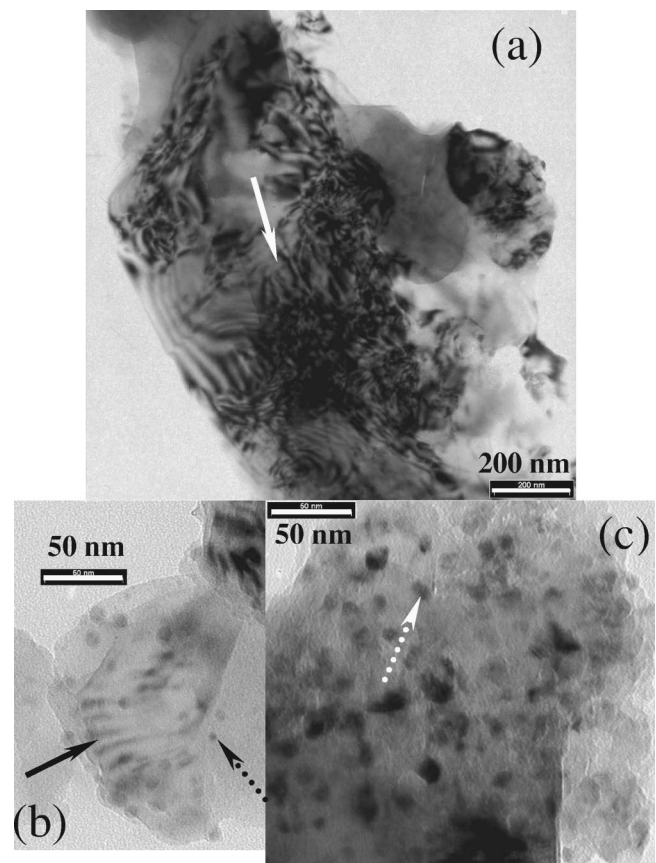


FIG. 7. TEM images of the  $x=0.2$  (a, b) and  $x=0.5$  (c) samples. A high dislocation density within grains is shown in (a). Dislocations and round shape inclusions are present within each grain (b). The number of inclusions increases with the doping level (c). The solid and dotted arrows mark dislocations and inclusions, respectively.

dislocations,<sup>23</sup> which can hardly provide strong pinning in high fields. Therefore, the high density of the dislocations induced by the substitution and revealed by TEM is a strong intragranular source of pinning. The dislocation size is estimated to vary from 5 nm to 30 nm which, on average, is larger only by a factor of about 2 than the coherence length  $\xi$  in  $\text{MgB}_2$  superconductor.<sup>2,24</sup> This makes them perfect pinning sites, because each vortex line has the diameter of the normal core of  $2\xi(T)$ .

Another contributing source of pinning, as in the case of  $\text{Y}_2\text{O}_3$  doping,<sup>17</sup> is nonsuperconducting nanosize precipitates, the amount of which grows with increasing doping level, as evident by the XRD patterns (Fig. 1). Indeed, the TEM study shows 2 nm to 10 nm large round shaped particles, presumably  $\text{Mg}_2\text{Si}$ , existing within each  $\text{MgB}_2$  grain [Figs. 7(b) and 7(c)]. Note that the inclusions are on average one order of magnitude smaller than the SiC-particles initially added, indicating that the SiC is absolutely dissolved in the  $\text{MgB}_2$  “solvent.” Moreover, the amount of these inclusions increases with increasing doping level, in particular after  $x \approx 0.2$ . At lower doping, fewer inclusion particles are observed. The optimal  $J_c(H)$  dependence is reached for the sample with  $x=0.3$  (Fig. 6) when the volume fraction of the nonsuperconducting impurity  $\text{Mg}_2\text{Si}$  content was about 30% (Fig. 1). A further  $x$ -increase starts to worsen the  $J_c(H)$  be-

havior, and, at the same time, the  $a$ -axis of the crystal lattice parameter exhibits a quasiplateau within the experimental error (Fig. 2). This correlation indicates that the optimal  $J_c(H)$  behavior is reached when the substitution effect has reached saturation. Presumably, this is because at this stage the maximum quantity of dislocations and a rather high level of inclusions coexist, balanced with a reasonable amount of superconducting phase. Further B replacement leads to the gradual elimination of the superconducting phase and, hence, worsening of  $J_c(H)$  performance. The above arguments, together with the fact that inclusions alone<sup>17</sup> had a less pronounced effect than in our case, lead to a conclusion that at high fields substitution, inducing a strongly developed net of dislocations, is the dominating source of the pinning in the material, which is possibly aided by localized superconducting order parameter fluctuations.

Furthermore, the point-like round-shaped inclusions seen in Figs. 7(b) and 7(c) can be effective only at extremely high density of the inclusions and at rather high temperatures, since their pinning ability is of a “collective” nature due to their point-like action and because vortex lines have to be rather soft to be pinned by these defects. This also means that pinning by these defects would be weakened in high fields where the vortex–vortex interaction is very strong, making the vortex lattice more rigid, so that the point-like defects become ineffective. In contrast, the pinning ability of the dislocations (extended defects) in increasing field is not expected to become less pronounced, since extended lengths of vortices can be trapped in randomly oriented dislocations. This is an additional argumentation to favor the role of the dislocations. However, their pinning force also reduces in increasing temperature because their pinning efficiency would be influenced by the temperature dependent coherence length. The higher the temperature, the longer the coherence length, and the weaker the pinning, since the dislocation size remains unchanged. This temperature behavior is seen in the experiment: the lower the temperature, the better the performance of the high-field part of  $J_c(H)$  for the best doping performance ( $0.1 \leq x \leq 0.3$ ), which is compared to the behavior of the nondoped sample (Fig. 6). The same trend can be found in Fig. 8 in which the available irreversibility fields as a function of doping level are plotted for all the samples. Unfortunately, the upper field limitation in our experimental techniques did not allow us to measure  $H_{irr}$  for some samples at  $T \leq 10$  K, since the  $H_{irr}$  increase for the samples having doping levels within  $0.1 \leq x \leq 0.3$  was too large.

A puzzling situation is imposed by the lowest doping level sample having  $x = 0.04$ . It shows  $J_c(H)$  behavior which is worse than most of the other samples except the one with the highest “superconducting” doping level  $x = 0.8$ . Similar behavior was observed in our preceding work,<sup>20</sup> but it remained unexplained. This behavior is also clearly seen in Fig. 8. There is a minimum at  $x = 0.04$ , which is the easiest to notice for  $T = 30$  K. We speculate that because the level of substitution was too small, neither a sufficiently large density of dislocations nor sufficient inclusions could be formed. On the other hand, the doping did cause a significant crystal lattice distortion, which might have led to strongly distorted

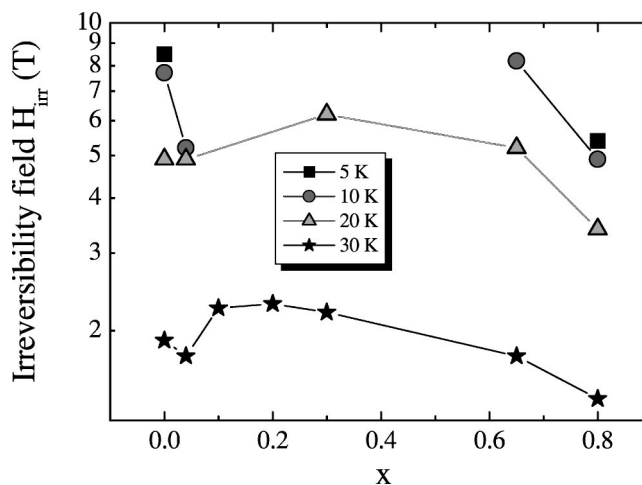


FIG. 8. The irreversibility field as a function of  $x$  for different temperatures. At lower temperatures  $T \leq 10$  K,  $H_{irr}$  for the samples within the  $0.1 \leq x \leq 0.3$  doping range is increased beyond the field range accessible by our measuring equipment. Note the logarithmic scale of  $H_{irr}$ .

supercurrent paths (for example due to a higher level of porosity) leading to the poor  $J_c(H)$  behavior observed.

#### IV. CONCLUSION

The main result of this work is the introduction of atomic substitutions of both Si and C in the crystal lattice of the  $MgB_2$  superconductor, as indirectly evidenced by a combination of numerous structural and magnetic experiments. This co-substitution was likely to be enabled due to the counterbalanced atomic size of Si and C, on average nearly coinciding with the sizes of B. Substitution was shown to prevail up to the rather high doping level  $x \approx 0.3$  in the  $MgB_{2-x}(SiC)_{x/2}$  composition. At higher doping levels the doping results in impurities, which eventually suppress the bulk superconductivity. The substitution was shown to very strongly improve  $J_c(H)$  dependence at high applied fields. We have suggested a pinning mechanism explaining this improvement, in which the main intragranular ingredients are the dominating contribution of a large number of dislocations induced by substitution effects and the secondary contribution of the nano-inclusions.

After the submission of this manuscript, we verified our results by preparing and characterizing a similar set of SiC-doped samples through a slightly different preparation method. This preparation method led to even more significant enhancement of  $J_c(H)$  than that presented in this work. These results are reported elsewhere.<sup>25</sup>

#### ACKNOWLEDGMENTS

The authors thank E. W. Collings, R. Neal, T. Silver, M. J. Qin, M. Sumption, and M. Tomsic for their helpful discussions. This work was supported by the Australian Research Council, Hyper Tech Research Inc., Ohio, Alphatech International Ltd., New Zealand, and the University of Wollongong.

<sup>1</sup>J. Nagamatsu, N. Nakagawa, T. Muranaka, Y. Zenitani, and J. Akimitsu, *Nature (London)* **410**, 63 (2001).

<sup>2</sup>C. Buzea and T. Yamashita, *Supercond. Sci. Technol.* **14**, R115 (2001).

- <sup>3</sup>T. Takenobu, T. Ito, D. H. Chi, K. Prassides, and Y. Iwasa, *Phys. Rev. B* **64**, 134513 (2001).
- <sup>4</sup>W. Mickelson, J. Cumings, W. Q. Han, and A. Zettl, *Phys. Rev. B* **65**, 052505 (2002).
- <sup>5</sup>M. R. Cimberle, M. Novak, P. Manfrinetti, and A. Palenzona, *Supercond. Sci. Technol.* **15**, 43 (2002).
- <sup>6</sup>W. Goldacher, S. I. Schlachter, S. Zimmer, and H. Reiner, *Supercond. Sci. Technol.* **14**, 787 (2001).
- <sup>7</sup>H. L. Suo, C. Beneduce, M. Dhalle, N. Musolino, J. Y. Genoud, and R. Flukiger, *Appl. Phys. Lett.* **79**, 3116 (2001).
- <sup>8</sup>G. Grasso, A. Malagoli, C. Ferdeghini, S. Roncallo, V. Braccini, M. R. Cimberle, and A. S. Siri, *Appl. Phys. Lett.* **79**, 230 (2001).
- <sup>9</sup>B. A. Glowacki, M. Majoros, M. Vickers, J. E. Evetts, Y. Shi, and I. McDougall, *Supercond. Sci. Technol.* **14**, 193 (2001).
- <sup>10</sup>S. Jin, H. Mavoori, and R. B. van Dover, *Nature (London)* **411**, 563 (2001).
- <sup>11</sup>S. Soltanian, X. L. Wang, I. Kusevic *et al.*, *Physica C* **361**, 84 (2001).
- <sup>12</sup>Y. Takano, H. Takeya, H. Fujii, H. Kumakura, T. Hatano, K. Togano, H. Kito, and H. Ihara, *Appl. Phys. Lett.* **78**, 2914 (2001).
- <sup>13</sup>C. B. Eom, M. K. Lee, J. H. Choi *et al.*, *Nature (London)* **411**, 558 (2001).
- <sup>14</sup>Y. Bugoslavsky, L. F. Cohen, G. K. Perkins, M. Polichetti, T. J. Tate, R. G. William, and A. D. Caplin, *Nature (London)* **411**, 561 (2001).
- <sup>15</sup>Y. Zhao, Y. Feng, C. H. Cheng, L. Zhou, Y. Wu, T. Machi, Y. Fudamoto, N. Koshizuka, and M. Murakami, *Appl. Phys. Lett.* **79**, 1154 (2001).
- <sup>16</sup>Y. Feng, Y. Zhao, Y. P. Sun, F. C. Liu, B. Q. Fu, L. Zhou, C. H. Cheng, N. Koshizuka, and M. Murakami, *Appl. Phys. Lett.* **79**, 3983 (2001).
- <sup>17</sup>J. Wang, Y. Bugoslavsky, A. Berenov, L. Cowey, A. D. Caplin, L. F. Cohen, and J. L. M. Driscoll, *Appl. Phys. Lett.* **81**, 2026 (2002).
- <sup>18</sup>D. C. Larbalestier, M. O. Rikel, L. D. Cooley *et al.*, *Nature (London)* **410**, 186 (2001).
- <sup>19</sup>S. X. Dou, X. L. Wang, J. Horvat, D. Milliken, A. H. Li, K. Konstantinov, E. W. Collings, M. D. Sumption, and H. K. Liu, *Physica C* **361**, 79 (2001).
- <sup>20</sup>S. X. Dou, A. V. Pan, S. Zhou, M. Ionescu, H. K. Liu, and P. R. Munroe, *Supercond. Sci. Technol.* **15**, 1587 (2002).
- <sup>21</sup>X. L. Wang, S. Soltanian, J. Horvat, M. J. Qin, H. K. Liu, and S. X. Dou, *Physica C* **361**, 149 (2001).
- <sup>22</sup>See, for example, V. M. Pan and A. V. Pan, *Fiz. Nizk. Temp.* **27**, 991 (2001) [*Low Temp. Phys.* **27**, 732 (2001)], and references therein.
- <sup>23</sup>Y. X. Chen, D. X. Li, and G. D. Zhang, *Mater. Sci. Eng., A* **337**, 222 (2002).
- <sup>24</sup>D. K. Finnemore, J. E. Ostenson, S. L. Bud'ko, G. Lapertot, and P. C. Canfield, *Phys. Rev. Lett.* **86**, 2420 (2001).
- <sup>25</sup>S. X. Dou, S. Soltanian, J. Horvat, X. L. Wang, S. H. Zhou, M. Ionescu, H. K. Liu, P. Munroe, and M. Tomsic, *Appl. Phys. Lett.* **81**, 3419 (2002).